Techniques for monitoring of benthic primary production

21 december 2021

Verantwoording

Titel	Techniques for monitoring of benthic primary production
Opdrachtgever	Deltares
Projectleider	Melanie Boonstra
Auteur(s)	Tisja Daggers
Projectnummer	1283684
Aantal pagina's	24
Datum	21 december 2021
Handtekening	Ontbreekt in verband met digitale verwerking.
	Dit rapport is aantoonbaar vrijgegeven.

Colofon

TAUW bv
Australiëlaan 5
Postbus 3015
3502 GA Utrecht
T +31 30 28 24 82 4
E info.utrecht@tauw.com

Kenmerk R001-1283684DDT-V02-efm-NL

Inhoud

1 Introduction 4
1.1 Scope 4
2 *In situ* and *ex situ* measurement techniques 5
2.1 PAM fluorescence-based techniques 5
2.2 ^{14}C-incubations (slurries) 7
2.3 O_2-electrode and -optode measurements 7
2.4 CO_2 chambers 8
2.5 Summary 8
3 Remote sensing-based techniques 10
3.1 Quantification of benthic primary production 11
3.2 Quantification of MPB biomass 13
3.3 Quantification of photosynthetic parameters 14
3.4 Quantification of the sediment mud content 15
4 Next steps 16
5 Benthic primary production data 17
5.1 Data Méléder et al. (2018) 17
5.2 Data Méléder et al. (2020) 17
5.3 Data and scripts Daggers et al. (2018) 17
6 References 20

1 Introduction

1.1 Scope

This document presents a state-of-the-art review of methods to quantify benthic primary production in estuaries. The advantages and disadvantages of each method are discussed, including their assumptions and uncertainties in measurements. The review includes field and remote sensing measurement techniques.

The review is intended to select a method to validate a benthic primary production model of the Westerschelde (The Netherlands).

Benthic primary production in the Westerschelde

Benthic primary production in the Westerschelde is mainly associated with the presence of benthic microalgal communities or microphytobenthos (MPB) (Kromkamp et al. 1995). In temperate marine areas, MPB is mostly dominated by benthic diatoms (Meleder et al., 2007; Underwood and Kromkamp, 1999). Macroalgae contribute less than 5% to the total benthic primary production of the Westerschelde (Nienhuis, 1992). Macroalgae mainly occur on artificial rocky substrates in the Westerschelde and do not contribute significantly to the diet of primary consumers inhabiting these rocky substrates (Riera et al. 2004).

Due to the high water turbidity and associated relatively shallow photic zone of the Westerschelde (e.g. Z_{eu}: 0.88-1.80; Kromkamp et al., 1995; Z_{eu}: 0.44, Van der Wal et al. 2010), it is generally assumed that benthic primary production in the subtidal zone is negligible. Therefore, (published) measurements of benthic primary production in the subtidal zone of the Westerschelde are scarce/not available. It can be assumed that intertidal benthic primary production forms the main component of total benthic primary production of the Westerschelde (Kromkamp et al. 1995). In water bodies with generally lower water turbidities, subtidal benthic primary production can form a significant part of total benthic primary production (e.g. 12-20% in the Bay of Brest; Longphuirt et al. 2007).

MPB primary production is characterized by a high degree of spatial and temporal heterogeneity, which poses a common problem in studying MPB primary production rates (Karsten et al. 2019). MPB displays heterogeneity from the micro scale (10 to 1000 cm^2) to macro scale (100 to 10000 m^2) in terms of abundance and community composition (Saburova et al. 1995). As *in situ* and *ex situ* measurement techniques can provide a limited number of replicates, airborne and satellite remote sensing is being used increasingly to upscale those measurements (e.g. Daggers et al. 2018; Méléder et al. 2018; Méléder et al 2020).

Available *in situ* and *ex* situ measurement techniques will be described in the next chapter (ch. 2), which is followed by a description of remote sensing techniques to obtain benthic primary production (ch. 3). In chapter 4, advice will be given on how to obtain a complete validation dataset for the Westerschelde and in chapter 5, published scripts and datasets will be provided to obtain benthic primary production.

2 *In situ* and *ex situ* measurement techniques

In this chapter, commonly used *in situ* and *ex situ* measurement techniques are described. The described techniques include PAM fluorescence-based techniques, ^{14}C-incubations (slurries), O_2-electrode and -optode measurements and CO_2 chambers. In paragraph 2.5, advantages and disadvantages of each technique will be summarized.

2.1 PAM fluorescence-based techniques

Due to the highly variable nature of benthic primary production, there has been an increase in research on rapid and non-intrusive methods such as Pulse Amplitude Modulation (PAM) fluorometry (Morelle et al. 2018; Frankenbach et al. 2020) and oxygen electrodes (Serodio, 2003). Photosynthetic activity can be measured *in situ* or *ex situ* using PAM fluorometry.

Chlorophyll fluorescence is, along with heat dissipation, a by-product of photosynthesis and provides an indicator of all levels of photosynthesis. A PAM fluorometer generates saturating light pulses, before (F_v) and after (F_m') which fluorescent light emitted by algae is recorded. F_v/F_m' gives the effective yield of photosystem II photochemical energy. From the effective yield, the relative electron transport rate (rETR) and electron transport rate (ETR) can be calculated. Rapid light curves (RLC's) can be constructed to obtain an estimate of the ETR at increasing light intensities, which can be fitted to various models (e.g. Jassby and Platt, 1976; Eilers and Peeters, 1988). From the fitted models, photosynthetic parameters such as the photosynthetic efficiency (α), photosynthetic capacity (P_{max}) and optimal light intensity (E_{opt}) can be derived. The rETR or ETR can be converted to carbon fixation rates using a conversion factor (e.g. fig. 1 from Migné et al. 2007; Barranguet and Kromkamp, 2000; Daggers et al. 2018).

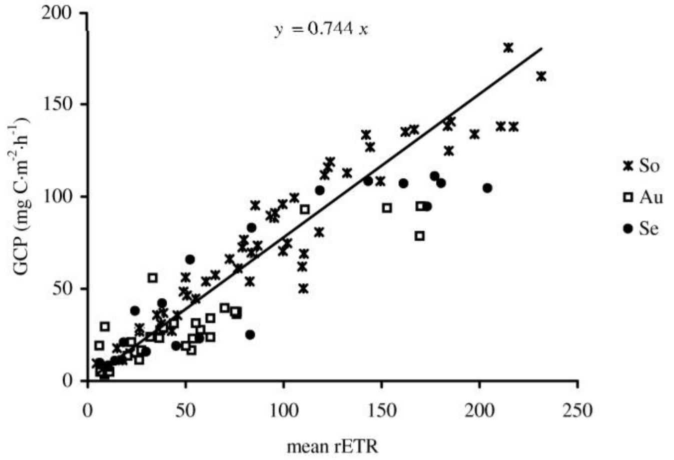

Fig 1. Gross community primary production (mg C m^{-2} h^{-1}) retrieved from ^{14}C-incubations plotted against mean relative electron transport rate (rETR; PAM fluorometry) measured in the Somme (So), Authie (Au) and Seine (Se). A conversion rate of 0.744 was forced through the origin (n=106, r=0.928, $P < 0.001$). Figure from Migné et al. (2007).

The conversion factor is not significantly different among seasons but shows variability (range ~0.015-0.11, μ=0.043), likely due to diurnal variation in photosynthesis or spatial patchiness of MPB (Barranguet and Kromkamp, 2000). Frankenbach et al. (2020) converted ETR rates to carbon fixation rates from hourly rates of O_2 evolution. The number of electrons required for evolution of 1 molecule of O_2 were shown to vary between 3 and 6 e O_2^{-1} for dominant phytoplankton and microphytobenthos species in the Ria de Aveiro (Vidal et al. 2017; Frankenbach et al. 2020). O_2 evolution can be converted to carbon fixation rates using the commonly accepted value of 1.1 mol C mol O_2 (Kromkamp et al. 2008). Serodio (2003) reported that 84.3 to 91.4% of variation in benthic primary production measured with oxygen electrodes could be explained by production calculated using fluorescence parameters.

Diving-PAM or Mini-PAM's (Walz GmbH, Germany) are frequently used to measure *in situ* photosynthetic activity using rapid light curves (Kromkamp et al. 2020). The optical fiber of the instrument is placed 4 mm perpendicular above the sediment surface in a dark chamber. After dark acclimation, rapid light curves are constructed using eight actinic increasing light levels, with 30s intervals (Daggers et al. 2018; Kromkamp et al. 2020). The length of dark acclimation varies between studies, as approximately 15 min is necessary to reach oxidation of the Quinone pool but downward migration initiates after ~5 min of dark acclimation (Perkins et al. 2010; Morelle et al. 2021).
Using an Imaging-PAM, the F_0, a fluorescence-based indicator for MPB biomass, and photosynthetic parameters can be measured *ex situ* on a 2D-grid. Application of this technique can visualize spatial variability in photosynthetic parameters on the microscale (Morelle et al. 2021).

PAM measurements are influenced by light attenuation, which depends mainly on the vertical profile of MPB (chl-a) within the sediment, vertical migration of MPB during performance of the rapid light curve and grain size. Morelle et al. (2018) developed a tool to correct photosynthetic parameters and primary production for these factors, and found that without correction ETR-values were mainly underestimated in relatively muddy sediments. The algorithm is available on request.

2.2 ^{14}C-incubations (slurries)

CO_2 -uptake can be measured by quantifying the incorporation of labelled ^{14}C in algae *ex situ* using a photosynthetron (Barranguet and Kromkamp, 2000). This provides the potential primary production, as the sediment sample is brought into suspension in filtered seawater. Hereby, vertical gradients present within the sediment that may limit benthic primary production are removed (e.g. gradients in nutrient, CO_2 and light availability). Barranguet et al. (1998), however, found a good agreement between carbon uptake values and gross production rates calculated with microelectrodes, with underestimations of production rates based on ^{14}C-incubations in periods of highest production (spring-summer). However, the number of recent applications of the method appears to be limited (e.g. Daggers et al. 2018; Jacobs et al. 2021).

2.3 O_2-electrode and -optode measurements

Benthic primary production can be derived from the total oxygen flux from the photic zone within the sediment or in the overlying water. An advantage of measuring the oxygen flux in the overlying water, is the fact that it gives an integrated value of benthic primary production. Total oxygen flux measurements within the sediment may be more sensitive to MPB spatial variability. Oxygen production can be measured using the light-dark method (Kromkamp & Forster, 2006) or photosynthesis-irradiance curves (Hoffmann et al. 2019). Hoffmann et al. (2019) constructed light-photosynthesis curves by measuring oxygen in the overlying water of collected sediment cores. The measured oxygen production rates can subsequently be converted to carbon sequestration (mg C m^{-2} h^{-1}) using a factor of 0.32 (Wolfstein et al., 2000).

Oxygen concentrations can be measured using oxygen electrodes (e.g. Kwon et al. 2021) or optodes. Karsten et al. (2021) report that oxygen optodes provide a number of advantages over conventional measurement techniques (e.g. Winkler-method or Clark-electrode), as i) optodes show an enhanced sensitivity for oxygen at low concentrations and ii) are not negatively influenced by hydrogen sulfide (Kühl & Polerecky, 2008), which is often present in sediments with high organic matter contents, and iii) they do not consume oxygen. Oxygen optodes and microelectrodes are generally applied *ex situ* (e.g. Kuriyama et al. 2021) are usually used for research and not for monitoring because of the relatively long duration of each measurement (Kromkamp & Philippart, 2015). Denis et al. (2012) performed *in situ* microprofile measurements with an automated portable unit (Miniprofiler MP4; Unisense™; Denis & Desreumaux, 2009), containing three oxygen microsensors. Applications of oxygen microelectrodes *in situ* are limited, likely due to the relatively long time needed to finish one vertical profile (Hawes et al. 2014).

2.4 CO_2 chambers

Using CO_2-chambers CO_2 consumption is measured *in situ* or *ex situ* by placing a closed-off transparent chamber over the sediment. By measuring the CO_2-concentration in the chamber using an infrared gas analyzer, net primary production can be quantified (e.g. Migné et al. 2007; Drylie et al. 2018; Méléder et al. 2020). Using dark chambers, respiration can be quantified. Acclimation of approximately 30 min is needed prior to performing dark incubations (Drylie et al. 2018). Summing up net primary production and respiration, results in an estimate of the gross primary production (GPP). CO_2 chambers provide an integrated value of primary production of the benthic community. Advantages of the method are that it's less sensitive to small-scale variability in MPB production and it leaves vertical gradients intact (Kromkamp, 2006). A disadvantage is the relatively long time need to perform one measurement (30 min per light or dark incubation and 30 min dark acclimation, Méléder et al. 2020).

2.5 Summary

The advantages and disadvantages of different techniques to measure benthic primary production are summarized in table 1.

Table 1. Summary of advantages and disadvantages of measurement techniques.

Techniques	Application	Advantages	Disadvantages
Diving-PAM or Mini-PAM	*In situ* or *ex situ* on the sediment	-non-intrusive -relatively rapid	-the relation between ETR and carbon fixation measured using 14C-incubations shows variability (range ~0.015-0.11, μ=0.043; Barranguet and Kromkamp, 2000) -the relation between ETR and O_2 evolution varies up to a factor 2 (e.g. Frankenbach et al. 2020) -Measurements are influenced by light attenuation and downward migration of MPB during RLC's. Morelle et al. (2018) developed a tool to correct for these factors.
Imaging-PAM	*Ex situ* on the sediment	-2D visualization of biomass and photosynthetic parameters (e.g. Morelle et al 2021)	See above.
^{14}C-incubations	*In situ* or *ex situ* on a sediment sample brought into suspension	-direct measurement of carbon fixation -Barranguet et al. (1998) found a good agreement between carbon uptake values and gross production rates calculated with microelectrodes (Clark-electrodes)	-sediment sample is brought into suspension, which removes vertical gradients in e.g. light availability present in a natural situation

Techniques	Application	Advantages	Disadvantages
Oxygen electrodes – light dark method	*In situ* or (usually) *ex situ* in the sediment.	-results are relatively easy to interpret	- equal respiration in light and dark assumed, which may not always be the case for diatoms (Kromkamp and Philippart, 2015). -can't be normalized for light conditions -measuring over a depth gradient is time consuming -cannot easily be interpolated to other days (measured at one light intensity)
	In situ or (usually) *ex situ* in the overlying water.	-relatively rapid -vertical gradients within the sediment remain intact -not sensitive to small-scale spatial patchiness of MPB	- equal respiration in light and dark assumed, which may not always be the case for diatoms (Kromkamp and Philippart, 2015). -can only be performed *ex situ,* as oxygen needs to be measured in a closed off system -cannot easily be interpolated to other days (measured at one light intensity) -underestimates true production, because the downward flux of O_2 into the sediment is not measured (Kromkamp and Philippart, 2015).
Oxygen electrodes – photosynthesis-irradiance curves	*In situ* or (usually) *ex situ* in the sediment.	-relatively simple compared to the light dark method (Kromkamp and Philippart, 2015).	-measuring over a depth gradient is time consuming -sensitive to small scale spatial patchiness -sediment porosity needs to be determined
	In situ or (usually) *ex situ* in the overlying water.	-relatively rapid -vertical gradients within the sediment remain intact -not sensitive to small-scale spatial patchiness of MPB	-can only be performed *ex situ,* as oxygen needs to be measured in a closed off system -underestimates true production, because the downward flux of O_2 into the sediment is not measured
Oxygen optodes – light dark method	*In situ* or (usually) *ex situ* in the sediment.	-higher sensitivity than microelectrodes at low oxygen concentrations -optodes don't consume O_2, are suitable for prolonged incubations -not negatively influenced by hydrogen sulfide	-measuring over a depth gradient is time consuming -sensitive to small scale spatial patchiness -cannot easily be interpolated to other days (measured at one light intensity)

Techniques	Application	Advantages	Disadvantages
	In situ or (usually) *ex situ* in the overlying water.	-relatively rapid -higher sensitivity than microelectrodes at low O_2 concentrations -vertical gradients within the sediment remain intact -not sensitive to small-scale spatial patchiness of MPB -optodes don't consume O_2, are suitable for prolonged incubations	-can only be performed *ex situ,* as oxygen needs to be measured in a closed off system -underestimates true production, because the downward flux of O_2 into the sediment is not measured -cannot easily be interpolated to other days (measured at one light intensity)
Oxygen optodes – photosynthesis-irradiance curves	*In situ* or (usually) *ex situ* in the sediment.	-higher sensitivity than microelectrodes at low oxygen concentrations -optodes don't consume O_2, are suitable for prolonged incubations -not negatively influenced by hydrogen sulfide	-measuring over a depth gradient is time consuming
	In situ or (usually) *ex situ* in the overlying water.	-relatively rapid -higher sensitivity than microelectrodes at low oxygen concentrations -vertical gradients within the sediment remain intact -not sensitive to small-scale spatial patchiness of MPB -optodes don't consume O_2, are suitable for prolonged incubations	-can only be performed *ex situ,* as oxygen needs to be measured in a closed off system -underestimates true production, because the downward flux of O_2 into the sediment is not measured

3 Remote sensing-based techniques

The advent of an increasing number of hyperspectral sensors, such as Hyperion, EnMAP and PRISMA, has led to an increasing number of studies focusing on the detectability of MPB biomass, sediment properties (i.e. water content and grain size) and photosynthetic parameters from chlorophyll fluorescence (e.g. Magney et al. 2017) or hyperspectral information (e.g. Méléder et al. 2018). This information can subsequently be used to calculate benthic primary production (e.g. Daggers et al. 2018). The revisiting time and timing of the image collection is, however, an important variable to consider when selecting a satellite sensor for use in intertidal areas. For this reason, multispectral imagery is still being used frequently (e.g. Méléder et al. 2020). Only imagery collected during daytime low tides on (mostly) cloud free days with an almost zenithal sun are suitable for further analyses. When field calibration is performed, the acquisition day of the satellite imagery should be as close as possible to the field campaign day (Daggers et al. 2018; Méléder et al. 2018; Méléder et al. 2020).

Techniques to retrieve photosynthetic parameters, biomass and the silt content from satellite imagery are discussed below.

3.1 Quantification of benthic primary production

Méléder et al. (2020) developed a model to derive GPP from multispectral imagery. An algorithm to map GPP was developed using: (i) the Normalized Difference Vegetation Index (NDVI) to map spatial variability in MPB biomass, (ii) emersion time, irradiance and mud surface temperature derived from the physical model MARS-3D and (iii) photosynthetic parameters retrieved from photosynthesis-irradiance (P-E) curves using benthic chambers constructed under controlled irradiance and temperature conditions.

A season-specific P^b (GPP/NDVI) was calculated, namely for March (representative for the biomass peak), May (intermediary biomass) and July (low biomass). The tidal height and irradiance were simulated using the hydrodynamical model MARS-3D. It was assumed that MPB biomass establishes progressively at the sediment surface within 20 min after emersion, and migrates downward 20 min before immersion. The mud surface temperature (MST) was derived from the MST model of Savelli et al. (2018) and coupled to MARS-3D. The MST model is described in detail by Savelli et al. (2018) and requires measurements or assumptions on the water content and porosity of the sediment. Irradiance and MST were used to obtain the P^b at each time step, which was derived from the P-E model fitted on laboratory measurements of P-E curves using benthic chambers. MST was used to simulate temperature-related variations in the P^b following Blanchard et al. (1996). NDVI maps, combined with the P^b, were used to create maps of the GPP (averaged hourly over the emersion period and daily-integrated). The method was validated using *in situ* GPP measurements: *in situ* measured values varied from 4.8 ± 2.1 mg C m^{-2} h^{-1} in March to 6.3 mg C m^{-2} h^{-1} in July (Fig. 2). Remotely sensed GPP values varied from 2.2 ± 1.4 mg C m^{-2} h^{-1} in July to 7.8 mg C m^{-2} h^{-1} in March. The measured GPP values coincide with other measured MPB production values in temperate climates, where peak values are measured in summer (e.g. Goto et al. 2000; Montani et al. 2003; Wolfstein et al. 2000), indicating that photosynthetic rates relate to air temperature (Montani et al. 2003).

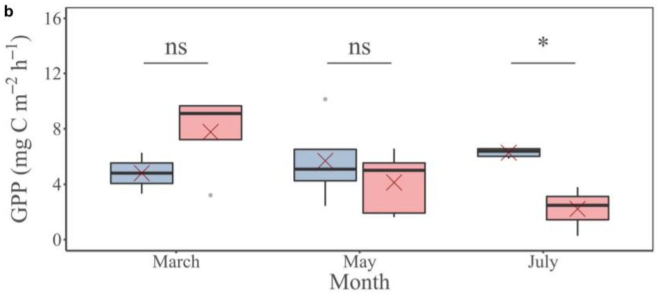

Fig. 2. GPP measured *in situ* (blue) and remotely sensed (red) at the Brouage mudflat (France) during three studied periods: March, May and July. Red crosses indicate the mean. Mann Whitney test, *p*-value: ns, $p > 0.01$; *$p \leq 0.01$; **$p \leq 0.001$; ***$p \leq 0.0001$. Figure from Méléder et al. 2020.

The method has been tested for a relatively muddy site, containing epipelic (migrating) diatoms. Sandy sediments generally contain non-motile (epipsammic) diatoms (Underwood & Kromkamp, 1999).

Daggers et al. (2018) proposed a method to derive benthic primary production from i) remotely sensed information on biomass and mud content, ii) ambient irradiance and temperature to obtain the P_{max} following Blanchard et al. (1996), iii) field measurements of photosynthetic parameters (α and E_{opt}) using PAM fluorometry and iv) a tide model. It was assumed that MPB migrate upward within the first hour after emersion (Paterson et al. 1998). The model could be optimized by use of the MST instead of ambient temperatures to obtain P_{max} (Daggers et al. 2018) or the P^b (Méléder et al. 2020). Furthermore, Méléder et al. (2020) suggested i) the use of benthic chambers instead of PAM fluorometry, as the conversion factor EE between ETR and carbon fixation rates may vary with season, site and species (Barranguet and Kromkamp, 2000) and ii) the direct use of the NDVI instead of a conversion of the NDVI to chl-a. The obtained primary production rates corresponded reasonably with field measurements (Fig. 3).

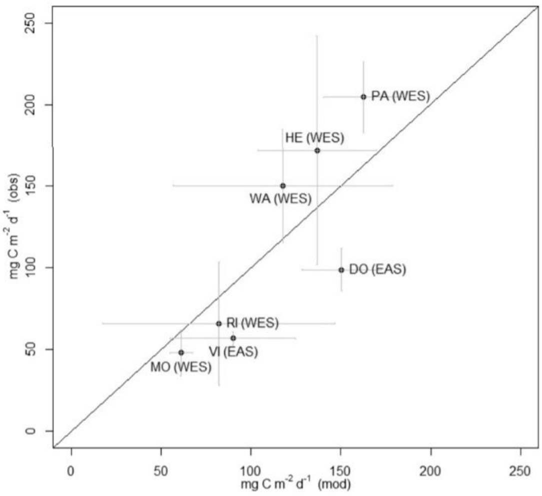

Fig. 3. Modelled and *in situ* average daily production (±SE) per site. Figure from Daggers et al. 2018. Sites in the Oosterschelde: Dortsman (DO, n = 2) and Viane (VI, n = 4). Sites in the Westerschelde: Hellegat (HE, n = 4), Molenplaat (MO, n = 4), Paulinapolder (PA, n = 4), Rilland (RI, n = 3) and Waardepolder (WA, n = 5). Figure from Daggers et al. 2018.

The photosynthetic efficiency was, both by Méléder et al. (2020) and Daggers et al. (2018) averaged per season and site. Further research is required on variability of this parameter over time (seasons and diurnal cycles; e.g. Kromkamp et al. 1998, Serodio et al. 2005) and space. Hyperspectral remote sensing may be able to capture the latter information (see paragraph 3.3).

3.2 Quantification of MPB biomass

As an alternative to the previously described methods, MPB primary production can be studied using remotely sensed information on (changes in) MPB biomass (e.g. Savelli et al. 2018). MPB biomass is also a prerequisite to calculate primary production following Méléder et al. (2020) or Daggers et al. (2018).
The NDVI is a widely used index to quantify MPB biomass on intertidal flats (Rouse et al. 1973; Brito et al. 2013; Daggers et al. 2018; Oiry and Barillé, 2021; Haro et al. 2022). The NDVI is, however, not specific for microphytobenthos and quantifies biomass of all photosynthesizing organisms. Several results have been reported regarding the proportions of variance (R^2) and/or degree of correlation (Pearson moment correlation) between the NDVI and chlorophyll-a concentration (r^2=0.75, Daggers et al. 2018; r^2=0.7, Brito et al. 2013) or chlorophyll-a content (r=0.72, Jesus et al. 2006). Jacobs et al. (2021) provide an overview of reported relationships between chl-a concentrations and the NDVI measured with a spectroradiometer or satellite sensor.
Jesus et al. (2006) emphasized that the vertical distribution of chlorophyll-a within the sediment depends on the sediment type (sand versus mud). This may cause slight differences in the relationship between the NDVI and chlorophyll-a concentrations in relatively muddy versus sandy sediments (sand, 1cm depth: r=0.74; mud, 1cm depth: r=0.68; Jesus et al. 2006). Barillé et al. (2011) found the NDVI to be relatively robust compared to other vegetation indices. Méléder et al.

(2020) highlights that the maximum NDVI value decreases with the spatial resolution of satellite imagery, due to dilution of the reflectance signal. Therefore, it may be preferred to use the NDVI as indicator for MPB biomass directly instead of applying a conversion to chl-a concentrations. The use of hyperspectral imagery may also overcome this scaling issue (Launeau et al. 2018).

Hyperspectral imagery allows the use of indices specific for MPB (MPBI; Méléder, 2010), diatoms (I_{diatom}) or euglenids ($I_{Euglenid}$) (Kazemipour et al., 2012). Kazemipour (2011) used a radiative transfer model to quantify chlorophyll-a concentrations using absorption at 673 nm (R^2=0.93). Kazemipour (2012) applied the same radiative transfer model, after separating the intertidal areas into diatom- or euglenid-covered sediments using the I_{diatom} and $I_{Euglenid}$:

$$I_{Diatom} = \frac{2R_{600}}{R_{459} + R_{673}} - 1$$

$$I_{Euglenid} = \frac{2R_{553}}{R_{600} + R_{495}} - 1$$

The indices allow distinction between pixels that are >50% covered by diatoms or euglenids, respectively.

3.3 Quantification of photosynthetic parameters

It has been suggested that passive fluorescence (solar-induced Chl fluorescence, SIF) could be used to obtain photosynthetic rates (Köhler et al. 2018; Mohammed et al. 2019). The technique has not yet been tested using photosynthetic organisms inhabiting intertidal areas. Magney et al. (2017) performed a laboratory experiment in which PAM measurements, leaf-level gas exchange and spectrally resolved fluorescence was measured on leaves of *Acer palmatum* and *Quercus lobata*. Strong relationships were found between variable fluorescence (F_λ, 670-850 nm) and PAM fluorescence parameters (F_t and F_m). The relationship is, however, dependent on the wavelength of the fluorescence emission curve, nonphotochemical quenching and photosystem II yield (photosynthetic efficiency). Therefore, further research is required on spatial, spectral and temporal dynamics of passive fluorescence in photosynthetic organisms (Magney et al. 2017; Mohammed et al. 2019). In addition, transferring laboratory results from variable fluorescence measurements to field situations should be done with caution, as growing environments, sampling protocols and sensor operating conditions may differ (Maxwell & Johnson, 2000; Mohammed et al. 2019).

Méléder et al. (2018) performed laboratory experiments to study the detectability of photosynthetic parameters measured with PAM fluorometry and from hyperspectral information (VIS-NIR reflectance; measured with a spectroradiometer). To this end, rapid light curves (RLC's) were performed using a Diving-PAM on diatom suspensions of an epipelic and epipsammic growth form to obtain the rETR and light use efficiency (LUE or photosynthetic efficiency). Subsequently, the suspension was deposited on a anisopore^{TM} polycarbonate membrane filter and spectral measurements were performed using an ASD FieldSpec3 spectrometer (300-2500 nm, spectral resolution 1 nm). They found that the light use efficiency can be derived from the $\delta\delta_{496/508}$ (MPB_{LUE}

index), from which the ETR can be calculated using irradiance and the average optical cross-section in the red domain of chl-a absorption (670-586 nm; fixed number, Méléder et al. 2013). The relationship between ETR and MPB_{LUE} is independent of MPB growth forms, which means the index can be applied to mixed natural assemblages. A similar index ($\delta\delta_{508}/\delta\delta_{630}$) tested on benthic diatom species has been proposed by Jesus et al. (2008). However, the relationship found by Jesus et al. (2008) was exponential, whereas Méléder et al. (2018) found a linear relationship between the index and ETR. According to Méléder et al. (2018) this could be explained by differing light conditions (light acclimation, duration and intensity) or a different chl-c content, which is species dependent. The latter possibility would support the use of the MPB_{LUE}, as it is species independent. The method has not yet been tested *in situ*, where cells may be self-shaded or migrate vertically within the sediment. The index would require a sensor with a band width of 15nm or smaller.

3.4 Quantification of the sediment mud content

The sediment mud content or silt content (% particles < 63 µm) derived from remote sensing may be used to obtain an estimate of the vertical light climate in sediments and the vertical distribution of MPB within the sediment, which can be used to calculate primary production (Daggers et al. 2018; Jesus et al. 2006). The sediment mud content can be derived from surface reflectance in the green and SWIR (R^2=0.4 for the Westerschelde) or a combination of surface reflectance in the green, SWIR and C-band SAR backscattering (R^2=0.45) (Van der Wal et al. 2007). The regression algorithms found by Van der Wal (2007) were consistent in time, making them suitable for time series analyses. The algorithms are specific for the Westerschelde. Daggers et al. (2018) used surface reflectance in the blue and infrared to estimate mud content (R^2=0.72) in the Westerschelde. The relationship was tested on two images and appeared to be less robust when applied to other imagery, which implies that calibration may be required for each image. Rainey et al. (2003) used a principal component analysis to obtain an estimate of the clay abundance from airborne imagery (R^2=0.79). The accuracy of the clay abundance estimate depended on exposure time of the tidal flats, which generally lowers the moisture content. Verpoorter et al. (2014) showed that using a spectral derivative-modified gaussian model the grain size can be separated from water content. Grain sizes of 35 µm (r^2_c=0.93), 45 µm (r^2_c=0.91) and 60 µm (r^2_c=0.96) could be predicted accurately. The algorithm to obtain grain size from gaussian and continuum parameters was tested using a laboratory experiment, in which sediment samples were dehydrated and measured using a spectroradiometer. The algorithm has not yet been tested *in situ*, which may generate somewhat different results due to an increased complexity of the geophysical properties (e.g. surface roughness) and composition (e.g. degree of sorting) of sediments (Verpoorter et al. 2014).

4 Next steps

Due to the heterogeneous nature of MPB primary production, it is advised to use remotely sensed information as validation of the benthic primary production model. The method developed by Méléder et al. (2020) or Daggers et al. (2018) can be used, or a combination. The method of Méléder et al. (2020) has the advantage that it does not require remotely sensed information of the mud content, which causes uncertainty in the resulting primary production values (remotely sensed information vs. sampled mud content: R^2=0.72; Daggers et al. 2018). The method of Méléder et al. (2020) could be adapted by using the method of Daggers et al. (2018) to obtain emersion versus immersion at each pixel instead of using the hydrodynamical model MARS-3D as proposed by Méléder et al. (2020). The required scripts to obtain production would need to be requested from the authors or adapted from scripts of Daggers et al. (2018).

When the method of Daggers et al. (2018) is used, the method could be optimized by using mud surface temperature instead of ambient temperature to obtain the Pmax following the temperature-Pmax relationship of Blanchard et al. (1998), as suggested by Méléder et al. (2020). The mud surface temperature can be derived from the model of Savelli et al. (2018). Mud surface temperatures are known to increase with 2-3 °C per hour (Guarini et al. 1997), while air temperatures do not display such extreme fluctuations. As Pmax is directly related to temperature, using a mud surface temperature model may significantly improve primary production estimates.
It is advised to calibrate the silt content for each separate satellite image when using the method of Daggers et al. (2018). By using the method of Daggers et al. (2018), spatial variability in the vertical light climate and the vertical distribution of MPB are accounted for, which has not been included in the method of Méléder et al. (2020). A sensitivity analysis showed that the mud content, from which the vertical distribution of MPB was derived following Jesus et al. (2006), caused an important part of the variability observed in MPB primary production.

The methods of Méléder et al. (2020) and Daggers et al. (2018) both require field calibration of P-E curves using a method of choice (PAM fluorometer or CO_2 chamber), to obtain an average value of the photosynthetic efficiency (α) and optimal light intensity (E_{opt}) per season. Measurements should be performed as close as possible in time to image acquisition. Using a PAM fluorometer, a larger number of measurements can be performed and the instrument is relatively easy in use. However, conversion to carbon fixation rates using a conversion factor is necessary, which causes some uncertainty (±75% of variance explained; Migné et al. 2007).
If available, photosynthetic parameters can be derived from hyperspectral imagery following Méléder et al. (2018) and validated using the collected P-E curves in the field. In this way, spatial variation in photosynthetic parameters can be accounted for. The method of Méléder et al. (2018) has, however, only been tested in a laboratory setting and has not yet been tested *in situ*.

5 Benthic primary production data

5.1 Data Méléder et al. (2018)

Available via https://figshare.com/articles/dataset/data_PlosOne_Meleder_2017_txt/5615746

5.2 Data Méléder et al. (2020)

Available via https://zenodo.org/record/3862068#.YZe8l9DMJPY.

5.3 Data and scripts Daggers et al. (2018)

Available via:
https://data.4tu.nl/articles/dataset/Supplementary_data_and_scripts_for_the_paper_A_model_to_assess_microphytobenthic_primary_production_in_tidal_systems_using_satellite_remote_sensing_including_Corrigendum_2019_/17032439/1

Folder 'Tide model'

All_gauges_WES.csv, All_gauges_OOS.csv
Water heights at tide gauges in the Westerschelde and Oosterschelde during the study period (March 11th 2015 to April 10th 2015). Tide gauge data can be downloaded here: https://waterinfo.rws.nl

Coord-waterbase_stations.txt
Spatial coördinates of the tide gauge stations where water heights were retrieved from.

Bathymetry Westerschelde (wschelde20151.img) and Oosterschelde (Oosterschelde_2013cm.img)
Bathymetry of the Westerschelde (31-12-2015) and Oosterschelde (30-12-2013), provided by Rijkswaterstaat. The spatial resolution of the grid is 2m.

L1_WES_noveg.txt, L1_OOS_noveg.txt
Text file containing the spatial coordinates of the pixels of interest (retrieved from Landsat-8 OLI image of 12-03-2015).

Folder 'Primary production model'

Lichtintensiteit_meetperiode.csv
Average hourly measurements of ambient irradiance retrieved from a LiCOr LI191 SA PAR quantum sensor connected to a LI-1000 data logger located at the roof of the nearby NIOZ institute, Yerseke, The Netherlands.

Temperature_knmi.csv
Ambient temperature was used to model the photosynthetic capacity (Ps) and was retrieved from a nearby weather station of the Royal Netherlands Meteorological Institute (KNMI) located at the mouth of the Westerschelde (Vlissingen, The Netherlands).

L2_WES_noveg.txt, L3_WES_noveg.txt, L4_WES_noveg.txt, L5_WES_noveg.txt
Reflectance of band 2, 3, 4 and 5 and spatial coordinates of each pixel retrieved from Landsat-8 OLI (12-03-2015).

Folder 'Field measurements'

Slib_chla_03042015.csv
Sediment samples of the upper 1cm of the sediment analyzed for chl-a, collected on the tidal flats of the Westerschelde in March and April 2015 (6 locations).

Slib_03042015_methooglaag.csv
Sediment samples of the upper 1cm of the sediment analyzed for grain size distributions, collected on the tidal flats of the Westerschelde in March and April 2015 (6 locations).

EP_pars0304_allplots.csv
PAM fluorescence measurements (light-response curves) on 6 tidal flats in the Westerschelde, collected in March and April 2015.

Lichtintensiteit_meetperiode.csv
Average hourly measurements of ambient irradiance retrieved from a LiCOr LI191 SA PAR quantum sensor connected to a LI-1000 data logger located at the roof of the nearby NIOZ institute, Yerseke, The Netherlands.

Emersion_WES_hour_plots_firsthour_excl.RData
A matrix containing information on emersion (1) or immersion (0) of each pixel in the study area, i.e. the tidal flats of the Westerschelde, during the study period (March 11th 2015 to April 10th 2015).

Scripts

Get_water_heights_allpixels_hourly_average.R
The script calculates the water height for each pixel of interest, using the three nearest tide gauges. Water heights at each pixel are calculated with inverse distance weighting. Using a bathymetry map of the Westerschelde, a matrix is constructed indicating whether a pixel is emersed or immersed at each time step within the study period. This matrix can be constructed with or without inclusion of the first hour after emersion of the sediment (see discussion in Daggers et al. 2018). The same calculation is performed for the locations of a number of (field) validation stations (emersion_plots032015.RData).

Required datasets:
Coord_waterbase_stations.txt
All_gauges_WES.csv
L1_WES_noveg.txt
Westerschelde_20151

PP_model_RS_2Dmap_NOVEG.R
The script calculates benthic primary production (mg C m^{-2} h^{-1}) for each pixel. The value represents an average of benthic primary production over a month, to account for spatial variation in emersion duration. Band 2, 3, 4 and 5 of Landsat-8 are required to calculate the NDVI, NDWI and the silt content using a linear regression formula. Air temperature data is required to derive the P_{max}. A matrix indicating emersion versus immersion (1/0) at each pixel is needed and can be retrieved from the script *Get_water_heights_allpixels_hourly_average.R.* Macroalgae and water were excluded using masks of NDVI < 3 and NDWI < 0, respectively. The K_d of the sediment was derived from the NDVI. The vertical distribution of chl-a within the sediment was related to the silt content. See Daggers et al. (2018) for a full description of the methodology.

Required datasets:
L2_WES_noveg.txt
L3_WES_noveg.txt
L4_WES_noveg.txt
L5_WES_noveg.txt
Temperature_knmi.csv
Lichtintensiteit_meetperiode.csv
Emersion_WES_hour_firsthour_excl_noveg_correct_bathy.RData

PP_model_fieldbased.R
The script calculates benthic primary production (mg C m^{-2} h^{-1}) for each sampling station. The value represents an average of benthic primary production over a month, to account for spatial variation in emersion duration. Photosynthetic parameters were measured using a Mini PAM*.* Sediment samples were collected at each sampling station and analyzed for grain size distribution (including the mud content) and chl-a concentrations. The K_d of the sediment was derived from the chl-a concentration. The vertical distribution of chl-a within the sediment was related to the mud content. See Daggers et al. (2018) for a full description of the methodology.

Required datasets:
Slib_chla_03042015.csv
Slib_03042015_methooglaag.csv
EP_pars0304_allplots.csv
Lichtintensiteit_meetperiode.csv
Emersion_WES_hour_plots_firsthour_excl.RData

6 References

Barranguet, C. et al., 1998. Factors controlling primary production and photosynthetic characteristics of intertidal microphytobenthos. Marine Ecology Progress Series 173, 117-126

Barranguet, C. & Kromkamp, J., 2000. Estimating primary production rates from photosynthetic electron transport in esuarine microphytobenthos. Marine Ecology Progress Series 204, 39-52

Blanchard, G. F., 1996. Quantifying the short-term temperature effect on light-saturated photosynthesis of intertidal microphytobenthos. Marine Ecology Progress Series 134, 309-313

Brito, A. C. et al., 2013. Seasonality of microphytobenthos revealed by remote-sensing in a South European estuary. Continental Shelf Research 66, 83-91

Daggers, T. D. et al., 2018. A model to assess microphytobenthic primary production in tidal systems using satellite remote sensing. Remote Sensing of Environment 211, 129-145

Denis, L. & Desreumaux, P., 2009. Short-term variability of intertidal microphytobenthic production using an oxygen microprofiling system. Marine and Freshwater Research 60(7), 712-726

Drylie, T. P. et al., 2018. Benthic primary production in emeged intertidal habitats provides resilience to high water column turbidity. Journal of Sea Research 142, 101-112

Eilers, P.H. C. & Peeters, J. C. H., 1988. A model for the relationship between light-intensity and the rate of photosynthesis in phytoplankton. Ecological Modelling 42(3-4), 199-215

Frankenbach, S. et al., 2020. Synoptic spatial-temporal variability of the photosynthetic productivity of microphytobenthos and phytoplankton in a tidal estuary. Frontiers in marine science 7, 170

Goto, N. et al., 2000. Seasonal variation in primary production of microphytobenthos at the Isshiki intertidal flat in Mikawa Bay. Limnology 1, 133-138

Haro, S. et al., 2022. Microphytobenthos spatio-temporal dynamics across an intertidal gradient using Random Forest Classification and Sentinel-2 imagery. Science of the Total Environment 804, 149983

Hawes, I. et al., 2014. Estimating photosynthetic activity in microbial mats in an ice-covered Antarctic lake using automated oxygen microelectrode profiling and variable chlorophyll fluorescence. Limnology and Oceanography 59(3), 674-688

Hoffmann, R. et al., 2019. Implications of glacial melt-related processes on the potential primary production of a microphytobenthic community in Potter cove (Antarctica). Frontiers in Marine Science 6, 655

Karsten, U. et al., 2021. Benthic diatoms on sheltered coastal soft bottoms (Baltic Sea) – seasonal community production and respiration. Journal of Marine Science and Engineering 9(9), 949

Kazemipour, F. et al., 2012. Microphytobenthos biomass mapping using the optical model of diatom biofilms: application to hyperspectral images of Bourgneuf Bay. Remote Sensing of Environment 127, 1-13

Kromkamp, J. et al., 1995. Nutrients, light and primary production by phytoplankton and microphytobenthos in the eutrophic, turbid Westerschelde Estuary (the Netherlands). Hydrobiologia 311 (1-3), 9-19

Kühl, M. & Polerecky, L., 2008. Functional and structural imaging of phototrophic microbial communities and symbioses. Aquatic Microbial Ecology 53, 99-118

Kuriyama, K. et al., 2021. Microphytobenthic primary production on exposed coastal sandy sediments of the Southern Baltic Sea using ex situ sediment cores and oxygen optodes. Oceanologia 63, 247-260

Jacobs, P. et al., 2021 (preprint). Assessing biomass and primary production of microphytobenthos in depositional coastal systems using spectral information. BioRxiv

Jassby, A. D. & Platt, T., 1976. Mathematical formulation of the relationship between photosynthesis and light for phytoplankton. Limnology and Oceanography 21(4), 540-547

Jesus, B. et al., 2006. Effect of sediment type on microphytobenthos vertical distribution: modelling the productive biomass and improving ground truth measurements. Journal of Experimental Marine Biology and Ecology 332(1), 60-74

Jesus, B. et al., 2008. Detection of diatom xanthophyll cycle using spectral reflectance. Journal of Phycology 44, 1349-1359

Köhler, P. et al., 2018. Global retrievals of solar-induced chlorophyll fluorescence with TROPOMI: first results and intersensory comparison to OCO-2. Geophysical research letters 45(19), 10456-10463

Kromkamp, J. C. & Forster, R., 2006. Developments in microphytobenthos primary productivity studies. In: Kromkamp, J. C. et al. (eds). Functioning of microphytobenthos in estuaries. Royal netherlands Academy of Arts & Sciences (KNAW), Amsterdam, 9-30

Kromkamp, J. et al., 1995. Nutrients, light and primary production by phytoplankton and microphytobenthos in the eutrophic, turbid Westerschelde estuary (The Netherlands). Hydrobiologia 311, 9-19

Kromkamp, J. et al., 1998. Determination of microphytobenthos PSII quantum efficiency and photosynthetic activity by means of variable chlorophyll fluorescence. Marine Ecology Progress Series 162, 45-55

Kromkamp, J. et al., 2008. Estimating phytoplankton primary production in Lake Ijsselmeer (The Netherlands) using variable fluorescence (PAM-FRRF) and C-uptake techniques. Europena Journal of Phycology 43, 327-344

Kromkamp, J. & Philippart, C. J. M., 2015. Primaire productie in het Waddengebied: meten en berekenen. Koninklijk Nederlands Instituut voor Onderzoek der Zee

Kwon, B. et al., 2021. The relationship between primary production of microphytobenthos and tidal cycle on the Hwaseong mudflat, west coast of Korea. Journal of Coastal research 30(6), 1188-1196

Launeau, P. et al., 2018. Microphytobenthos biomass and diversity mapping at different spatial scales with a hyperspectral optical model. Remote Sensing 10, 716

Longphuirt, S. N. et al., 2007. Primary production and spatial distribution of subtidal microphytobenthos in a temperate coastal system, the Bay of Brest, France. Estuarine, Coastal and Shelf Science 74 (3), 367-380

Magney, T. S. et al., 2017. Connecting active to passive fluorescence with photosynthesis: a method for evaluating remote sensing measurements of Chl fluorescence. New Phytologist 215, 1594-1608

Maxwell, K. & G. N. Johnson, 2000. Chlorophyll fluorescence – a practical guide. Journal of Experimental Botany 51, 659-668

Méléder, V. et al., 2007. Spatiotemporal changes in microphytobenthos assemblages in a macrotidal flat (Bourgneuf bay, France). Journal of Phycology 43, 1177-1190

Méléder et al., 2010. Hyperspectral Imaging for mapping microphytobenthos in coastal areas. In: Maanan, M.R.E. (Ed.s), Geomatic solutions for coastal environments. Nova Science Publishers

Méléder et al., 2013. In vivo estimation of pigment composition and optical absorption cross-section by spectroradiometry in four aquatic photosynthetic micro-organisms. Journal of Photochemistry and Photobiology B: Biology 129, 115-124

Méléder et al., 2018. Microphytobenthos primary production estimated by hyperspectral reflectance. Plos one 13(5), e0197093

Méléder et al., 2020. Mapping the intertidal microphytobenthos gross primary production part I: coupling multispectral remote sensing and physical modeling. Frontiers in Marine Science 7, 520

Migné, A. et al., 2007. Photosynthetic activity of intertidal microphytobenthic communities during emersion: in situ measurements of chlorophyll fluorescence (PAM) and CO2 flux (IRGA) 1. Journal of Phycology 43(5), 864-873

Mohammed, G. H. et al., 2019. Remote sensing of solar-induced chlorophyll fluorescence (SIF) in vegetation: 50 years of progress. Remote Sensing of Environment 213, 111177

Montani, S. et al., 2003. Seasonal and interannual patterns of intertidal microphytobenthos in combination with laboratory and areal production estimates. Marine Ecology Progress Series 249, 79-91

Morelle, J. et al., 2018. A simple, user friendly tool to readjust raw PAM data from field measurements to avoid over- or underestimating of microphytobenthos photosynthetic parameters. Journal of Experimental Marine Biology and Ecology 503, 136-146

Morelle, J. et al., 2021. Contrasted impact of two macrofaunal species (*Hediste diversicolor* and *Scrobicularia plana*) on microphytobenthos spatial distribution and photosynthetic activity at microscale. Marine Environmental Research 163, 105228

Nienhuis, P. H., 1992. Eutrophication, water management, and the functioning of Dutch estuaries and coastal lagoons. Estuaries 15 (4), 538-548

Oiry, S. & Barillé, L., 2021. Using sentinel-2 imagery to develop microphytobenthos-based water quality indices in estuaries. Ecological Indicators 121, 107184

Paterson, D. M. et al., 1998. Microbiological mediation of spectral reflectance from intertidal cohesive sediments. Limnology and Oceanography 43(6), 1207-1221

Perkins et al., 2010. Vertical cell movement is a primary response of intertidal benthic biofilms to increasing light dose. Marine Ecology Progress Series 416, 93-103

Saburova, M. A. et al., 1995. Spatial structure of an intertidal sandflat microphytobenthic community as related to different spatial scales. Marine Ecology Progress Series 129, 229-239

Savelli, R. et al., 2018. On biotic and abiotic drivers of the microphytobenthos seasonal cycle in a temperate intertidal mudflat: a modelling study. Biogeosciences 15, 7243-7271

Serodio, J., 2003. A chlorophyll fluorescence index to estimate short-term rates of photosynthesis by intertidal microphytobenthos. Journal of Phycology 39, 33-46

Serodio, J. et al., 2005. Short-term variability in the photosynthetic activity of microphytobenthos as detected by measuring rapid light curves using variable fluorescence. Marine Biology 146, 903-914

Rainey, M. P. et al., 2003. Mapping intertidal estuarine sediment grain size distributions through airborne remote sensing. Remote Sensing of Environment 86(4), 480-490

Riera, P. et al., 2004. Utilization of food sources by invertebrates in a man-made intertidal ecosystem (Westerschelde, The Netherlands): a $\delta^{13}C$ and $\delta^{15}N$ study. Journal of the Marine Biological Association of the United Kingdom 84, 323-326

Underwood, G. J. C. & Kromkamp, J., 1999. Primary production by phytoplankton and microphytobenthos in estuaries. Advances in Ecological Research 29, 93-153

Van der Wal, D. & p. M. J. Herman, 2007. Regression-based synergy of optical, shortwave infrared and microwave remote sensing for monitoring of the grain-size of intertidal sediments. Remote Sensing of Environment 111, 89-106

Van der Wal, D & P. M. J. Herman, 2010. Spatial synchrony in intertidal benthic algal biomass in temperate coastal and estuarine ecosystems. Ecosystems 13 (2), 338-351

Verpoorter, C. et al., 2014. Visible, near-infrared spectrometry for simultaneous assessment of geophysical sediment properties (water and grain size) using the Spectral Derivative-Modified Gaussian Model. Journal of Geophysical Research: Earth Surface 119, 2098-2122

Vidal, T. et al., 2017. Phytoplankton dynamics in relation to seasonal variability and upwelling and relaxation patterns at the mouth of Ria de Aveiro (West Iberian Margin) over a four-year period. Plos One 12, e0177237

Wolfstein, K., et al., 2000. Seasonal dynamics of microphytobenthos biomass and photosynthetic characteristics in the northern German Wadden Sea, obtained by the photosynthetic light dispensation system. Estuarine and Coastal Shelf Science 51(5), 651-662